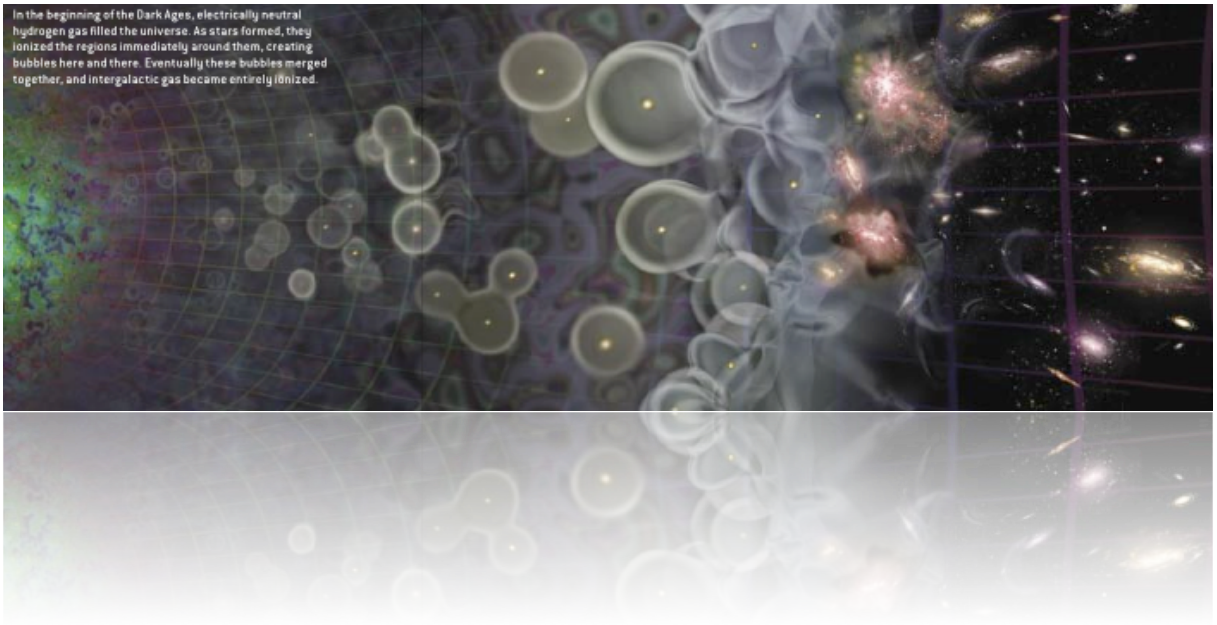

DEX
DARK AGES EXPLORER

A White paper for a low-frequency radio interferometer mission to explore the cosmological Dark Ages for the L2, L3 ESA Cosmic Vision program

24/05/2013

DEX Spokesperson:
Dr. Marc Klein Wolt

Department of Astrophysics - Research Institute for Mathematics, Astrophysics and Particle Physics, Radboud University Nijmegen

M.KleinWolt@astro.ru.nl
Heijendaalseweg 135, 6525 AJ Nijmegen, The Netherlands
T: +31 (0) 644130582

Authors:

Marc Klein Wolt (RU-Nijmegen, NL)
Garrelt Mellema (Stockholm University)
Leon Koopmans (RUG-Groningen, NL)
Heino Falcke (RU-Nijmegen, NL)
Willem Baan (ASTRON, IFR, NL)
Albert-Jan Boonstra (ASTRON, NL)
Leonid Gurvits (Jive, TUD-Delft, NL)
Mark Bentum (Univ. Twente, ASTRON, TUD, NL)
Chris Verhoeven (TUD- Delft, NL)
Joseph Lazio (JPL, USA)
Jack Burns (U. Colorado, USA),
Jan Bergman (IFR, Sweden)
Philippe Zarka (LESIA, OBSPM, CNRS)

Supporters of the DEX white paper:

Ian Crawford (Birkbeck College London)
Michael Garret (ASTRON, NL)
Jan-Erik Wahlund (IFR, Sweden)
Jean-Louis Bougeret (LESIA, OBSPM)
Amin Aminaei (RU, NL)
Hamid Pourshaghaghi (RU, NL)
James Carpenter (ESA/ESTEC, NL)
Kees van 't Klooster (ESA/ESTEC, NL)
Olaf Scholten (KVI, NL)
Stephane Corbel (CEA-AIM, Paris)
Huub Röttgering (Leiden Observatory, NL)
Jason Hessels (ASTRON, NL)
Ger de Bruyn (ASTRON, NL)

Dark Ages eXplorer - DEX

Summary

The Dark Ages eXplorer, DEX, is a low-frequency radio interferometer in space or on the moon, that will probe deep into the early universe and provide an unprecedented detailed view of the evolution of the first structures in the universe. DEX is sensitive in the 1-80 MHz regime which allows a complete view of the Dark Ages and Cosmic Dawn period, essentially covering the z=17-80 redshift regime. DEX will explore the Dark Ages and the Cosmic Dawn and observe the global neutral hydrogen (21 cm) emission and its variations on arcmin scales in order to constrain cosmological models on the evolution of the early universe, the onset of the epoch of reionization and basically constrain the models and predictions that will follow from the Planck mission. These issues form the holy grail of cosmology and the Dark Ages is the treasure-trove for Dark Matter and Early universe physicists. In addition, DEX will open up the last virtually unexplored frequency regime below 30 MHz, extending the view of LOFAR and SKA to the ultra-long wavelength regime that is not accessible from Earth, and among a wealth of science cases will provide high resolution low-frequency sky maps, constrain models on the jet power in radio galaxies, observe auroral emission from the large planets in our solar system and possibly find Jupiter-like exoplanets. DEX requires a large collecting area in the order of 10 km^2 (10^5 individual elements) and a location (preferably the lunar far-side) that provides shielding from man-made radio interference (RFI), absence of ionospheric distortions, and high temperature and antenna gain stability. The realization of large collecting area interferometers has been achieved on earth already (e.g. LOFAR and in the near future SKA) and the technique behind it is well developed (TRL 4-5). The realization in space or on the moon is a very challenging task. However, we are convinced that given the technology developments, especially in the areas of nano satellites, RF technology and low-power and high-performance computing, the construction of a large low-frequency radio array in space or on the moon is feasible in the 2020-2030 timeframe.

Introduction & Motivation

The Earth's turbulent ionosphere gives rise to “radio seeing'', making ground-based radio imaging of the sky difficult at frequencies below ~100 MHz. At even longer wavelengths below about 10-30 MHz one encounters the ionospheric cut-off where radio waves are reflected, permitting long-distance short wave transmission around the Earth, but making observations of the sky very difficult, which are finally prohibited by the ionosphere below ~10 MHz. Observing just above the cut-off, i.e., between ~10-50 MHz requires especially favorable geomagnetic and ionospheric conditions to obtain any decent images. The range below the cutoff is only readily observable from space. Hence, the dominant “low-frequency/long-wavelength'' regime for which ground-based telescopes are being designed is at frequencies above 30 MHz and wavelengths below 10 m. Even at this range, there are windows of strong interferences (e.g. FM frequencies, 80-100 MHz), which cannot be used for radio astronomy.

The best resolution achieved so far in the range below ~30 MHz is on the scale of a few degrees, but more typically of order tens of degrees. This compares rather unfavorably to the milli-arcsecond resolution that can be routinely obtained in very long baseline interferometry (VLBI) at higher radio frequencies. Hence, the low-frequency Universe is the worst charted part of the radio spectrum, and perhaps even of the entire electromagnetic spectrum. By today, only two kinds of maps of the sky have been made at frequencies below 30 MHz. The first are maps made from earth-based observatories such as the maps obtained by Cane & Whitham (1977), Ellis & Mendillo (1987) and Cane & Erickson (2001) of a part of the southern sky near the Galactic center and those made by the UTR-2 radio telescope (Braude et al., 2002). These have angular resolutions ranging from ~1 to 30 degrees. The second kind are maps obtained by the

RAE-2 satellite (Novaco & Brown, 1978) with angular resolution of 30 degrees or worse. None of these maps show individual sources other than diffusive synchrotron emission of the Galaxy, nor do they cover the entire sky.

To improve this situation and to overcome these limitations, space-based low-frequency telescopes are required for all observations below the ionospheric cutoff (Weiler, 1987; Weiler et al., 1988; Kassim & Weiler, 1990). This is also true for a significant part of the seeing-affected frequency range above the cutoff frequency (see Figure 1) where high-resolution and high-dynamic range observations are required, such as imaging of redshifted 21-cm emission of neutral hydrogen in the very early Universe (Carilli et al., 2007).

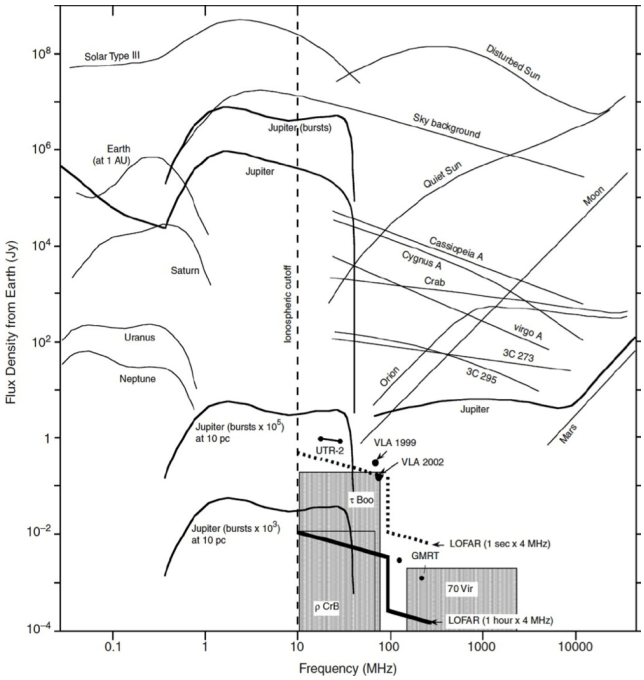

Figure 1: Spectra of astronomical radio sources detected from the Earth's vicinity (1 Jansky = 1 Jy = 10^{-26} $Wm^{-2}Hz^{-1}$). Galactic, extragalactic and solar spectra are adapted from (Kraus, 1986). Planetary spectra, corresponding to auroral radio emissions, are adapted from (Zarka, 1992). Jupiter's spectrum, which includes auroral and Io-induced decameter emissions, is from Zarka et al. (2004). Its average flux density is about 10^6 Jy, while peak flux densities reach or exceed 10^7 Jy during short-lived bursts. If all planetary emissions were normalized to the same observer distance of 1 AU, Jupiter's spectrum should be upscaled by x20, Saturn's by x100, Uranus' by x400, and Neptune's by x900, so that all are grouped within 2–3 orders of magnitude of each other. Jupiter's peak spectrum is reproduced with two different scalings to illustrate the possible radio spectrum of hot Jupiters. Shaded boxes are predictions from (Farrell et al., 1999). Sensitivities of UTR-2, VLA, GMRT and future LOFAR observations are indicated. The Earth's ionospheric cutoff is indicated at 10 MHz. (from Zarka, 2007)

So far, there have only been two space missions whose primary purpose was low-frequency radio astronomy: the Radio Astronomy Explorers (RAE) 1 and 2. It was a surprising finding of RAE-1 that the Earth itself is a strong emitter of low-frequency bursts, the so-called Auroral Kilometric Radiation (AKR) generated by solar-wind interactions with the Earth's magnetic field. This emission is so strong that RAE-2 was placed in a lunar instead of the originally planned terrestrial orbit to provide shielding from this natural terrestrial interference. The structure of the Galaxy's emission was only seen by RAE-2 at very low spatial resolution (with beam sizes between 37º × 61º and 220º × 160º) and fairly low signal-to-noise ratio. Due to the very limited angular resolution and the large power of AKR, it proved impossible to image any discrete sources directly.

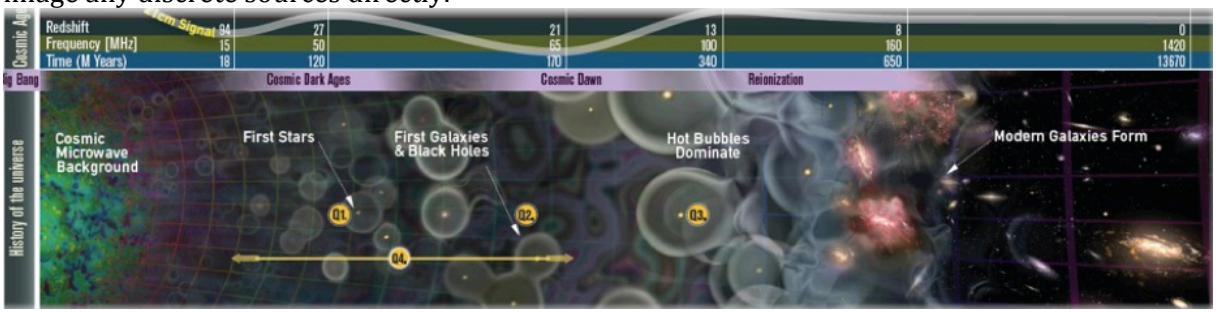

Figure 2: Formation history of the Universe. The Cosmic Dark Ages is the period with no stars and the only source of light is originating from the most abundant element, hydrogen. This H-I emission (21 cm line emission) is the only source of light that provides clues about the distribution of matter and dark matter in the early universe (Burns et al. 2012)

A fundamental question of current cosmological research is on the nature of structure formation in the Universe (for a review, see Ciardi and Ferrara, 2005): how is the observed distribution of visible matter created from the initial conditions just after the big bang, when matter and radiation were distributed

extremely smoothly, with density variations of just one part in 100,000? The Cosmic Microwave Background (CMB) radiation was emitted at z≈1200, about 400,000 years after the Big Bang, when the Universe had cooled off sufficiently for electrons and protons to recombine into neutral hydrogen atoms (Epoch of Recombination, EoR), allowing the background radiation to move freely without being scattered by the electrons and protons. At the same time, however, the Universe became opaque to visible light, because neutral hydrogen atoms absorb visible and infrared photons and re-emit them in random directions. Moreover, there were no sources of light in the Universe yet: the hydrogen and helium that were created in the big bang first had to cool in order to be able to clump together and form stars and galaxies. Hence, this era is called the ``cosmic dark ages'' in the redshift range z=30-1200 (Rees, 1999), see Figure 2.

Things only changed after the first stars, galaxies and active black holes had formed and emitted enough UV and X-ray photons to reionize the neutral hydrogen, allowing all radiation to pass freely. The time when this happened is called the Epoch of Reionization (EoR) and is believed to have occurred around z≈11, about 400 million years after the Big Bang, though it is at present not known whether the reionization happened more or less instantaneously, similar to a global phase transition, or was more or less spread out in time, depending on local conditions.

Throughout all these epochs hydrogen played a major role, emitting or absorbing the well-known 21-cm (1.4 GHz) line due to the spin-flip of the electron. This emission is redshifted by a factor 10 - 1000 due to the cosmological expansion and ends up in the frequency range from 140 - 1.4 MHz. When the hydrogen spin temperature is not coupled perfectly to the radiation temperature of the cosmic background radiation[1], but changed by other couplings with the surrounding matter and radiation, it can be seen against the cosmic background radiation in absorption or emission, depending on whether the spin temperature is lower or higher than the background radiation temperature. In this way, the cosmological 21-cm emission carries information about the evolution of the Universe.

Placing a radio antenna array at a large distance in space (e.g. Sun-Earth L2) or on the moon (e.g. in an eternally dark crater at the south (or north) pole) would provide perfect shielding from man-made radio interference (RFI), absence of ionospheric distortions, and high temperature and antenna gain stability that allows for sensitive and high resolution radio astronomy observations addressing a wealth of science cases – essentially opening up the last virtually unexplored frequency regime. In particular, such a low-frequency array would allow for the first time to probe the deep into the dark ages and observe the global neutral hydrogen (21 cm) emission and its variations in order to constrain cosmological models on the evolution of the early universe, the onset of the epoch of reionization and basically constrain the models that will come out of the Planck mission. These issues form the holy grail of cosmology and the Dark Ages is the treasure-trove for Dark Matter and Early universe physicists. This is a very challenging task that requires a large collecting area in space (or on the moon), very stable conditions and long integration times. However, we are convinced that given the technology developments, especially in the areas of nano satellites, RF technology and low-power and high-performance computing, the construction of a large low-frequency radio array in space or on the moon is feasible in the 2020-2030 timeframe.

DEX is a radio interferometer in space or on the moon, with a large collecting area in the order of 10 km^2, covering the low frequency regime between 1-80 MHz which is (partly) not accessible from earth and allows a complete view of the Dark Ages period essentially covering the z=17- 80 redshift regime. The realization of large collecting area interferometers has been achieved on earth already (e.g. LOFAR and in the near future SKA) and the technique behind it is well developed (TRL 4-5). For the space application DEX will rely on the expected rapid technology developments in the domain of nano-satellites, swarm-technologies, low-power & high-performance processing, and (optical) communication.

[1] Which is not a *microwave* background at those redshifts.

Science questions addressed by DEX

Primary science case: Dark Ages

After the epoch of recombination (redshift 1200) the Universe remained in neutral state until the large scale formation of galaxies released a sufficient number of ionizing photons into the intergalactic medium to ionize it. This process is thought to have completed by redshift 6 after which the only areas of neutral hydrogen in the Universe were to be found inside galaxies. Before the completion of the reionization, large regions of the Universe consisted of neutral hydrogen that, under favorable circumstances, produces an observable 21cm (1.4 GHz) signal that is observable today in the 1.2-200 MHz range due to the redshift. The whole period between z ~ 1200 and z ~ 6 can be divided into three different periods based on the nature of the physical processes at work and the 21cm signal generated (see also Figure 2):

1. Dark Ages (DA) - In this period which stretches from z ~ 1200 to ~ 30 the Universe was nearly completely neutral and no sources of light had formed. The evolution of matter was relatively simple as the only process at work was gravity. Due to the coupling of radiation and matter only the lower redshift part of this period is expected to generate 21cm absorption against the cosmic microwave background (z < 200). Models show that this signal is strongest around z~50 (~28 MHz) and becomes increasingly weaker as z~30 (~46 MHz) is approached.
2. Cosmic Dawn (CD) - In this period which stretches from z ~ 30 to ~15 the first dark matter halos collapsed and the baryons which followed in the collapse formed the first stars. The ultraviolet radiation from these stars changed the quantum state of the cold neutral hydrogen so that it once more produced an observable absorption against the CMB. Once a sufficient number of x-ray sources had heated the Inter-Galactic Medium (IGM) above the CMB temperature the signal changed from absorption to emission.
3. Epoch of Reionization(EoR) - From about z~15 to 6 the increasing number of ionizing photons escaping from galaxies started to substantially reduce the amount of neutral hydrogen in the IGM leaving it in a fully ionized state by the end of it. The still neutral areas of the heated IGM produced a 21cm emission signal (redshifted to ~90-200 MHz).

The first generation of low frequency radio telescopes on Earth such as LOFAR, MWA, PAPER, are targeting the EoR period (> 100 MHz) and are hoping to detect a signal within the next 5 years. The low frequency part of the Square Kilometer Array (SKA_Low) will target both the EoR and the CD periods (frequency range 50 – 300 MHz) and is expected to become operational around 2020. As explained above, Earth-based observations of even lower frequencies are challenging if not impossible and require space missions. ***Aiming for a frequency range of 1 – 80 MHz, DEX will target both the observable part of the DA period as well as early CD period.*** The science cases for these two periods are different and below we address them separately.

Dark Ages Science

During the DA gravitational collapse was mostly in the linear regime. Initially matter and radiation were sufficiently coupled to make the gas temperature equal to the CMB temperature, dropping as (1+z). Only around z~200 had the matter density dropped enough to allow the gas temperature to evolve independently, falling off adiabatically as $(1+z)^2$. The density was however still high enough to collisionally couple the quantum state of neutral hydrogen (expressed by the spin temperature T_s) to the gas temperature, causing the neutral hydrogen to produce an absorption signal against the CMB. As the density dropped even more, collisions became less and less effective and T_s tended towards T_{CMB}, causing the 21cm signal to disappear. Observations of the global 21cm absorption from the DA will test whether this simple scenario is correct. Deviations from the expected signal will be sensitive to a range of exotic heating processes such as decaying or annihilating dark matter, evaporating black holes, or cosmic strings. The physics behind the standard prediction is sufficiently simple that deviations will provide strong constraints on additional heating processes. The maximum absorption predicted lies around -50 mK.

Observations of the 21cm fluctuations, characterized by the power spectrum will provide unique cosmological data. The power spectrum will be dominated by the density fluctuations, just as for the CMB power spectrum. However, unlike the CMB which comes from a unique epoch, the DA 21cm signal

originates from a range of epochs and therefore contains ~10^6 more information than the CMB (Loeb & Zaldariagga, 2004). In addition, the DA 21cm signal can possibly probe the matter power spectrum at scales which are damped in the CMB (Loeb & Zaldariagga, 2004). The typical fluctuation amplitudes are predicted to lie in the range 0.1 to 1 mK.

Cosmic Dawn Science

Towards the end of the DA the 21cm absorption weakens because the collisional coupling to the gas temperature disappears. However, the appearance of the first generations of stars helps the 21 cm signal to reappear, due to the Wouthuysen-Field effect: absorption and re-emission of Ly-alpha photons by neutral hydrogen pushes the spin temperature back to the gas temperature. Initially the signal will be again in absorption as the gas temperature will still be below the CMB temperature. However, as X-ray producing sources develop (early X-ray binaries, supernova remnants and accreting black holes), this radiation will heat the IGM above the CMB temperature and push the signal into emission. The detailed timing of these processes is as yet unknown but models indicate that and absorption signal will be seen from about z~30 to 15 (46-89 MHz) after which the 21cm signal will be in emission (Pritchard & Loeb 2010). Observations of the global 21cm signal from the CD will establish when the first stars formed and when X-ray heating pushed the signal from absorption to emission, thus establishing among other things the rise of the first accreting black holes. The strength of the absorption signal could be as low as -200 mK, the emission signal has a maximum around 30 mK.

Observations of the 21cm power spectrum of fluctuations will probe the spatial variations in the above processes. Measurements of these variations can establish the distribution of the first stars and first X-ray sources. Substantial variations in the global star formation at this age have been predicted due to supersonic bulk flows in the neutral hydrogen on scales of a few cMpc with large scale variations on scales of ~100 cMpc (Tseliakhovich & Hirata 2010).
The spin temperature variations complicate the extraction of pure cosmological information from the power spectra. However, due to the presence of redshift space distortions it may still be possible to extract the cosmological matter power spectrum from the 21cm signal (Barkana & Loeb 2006). Models indicate that typical fluctuation amplitudes during the CD range from 1 to 10 mK.

Dark Ages signatures

The Dark Ages signature can typically be divided in three ways (e.g. Jester & Falcke, 2009):

- the Global Dark Ages signal – which is essentially the redshifted 21-cm line absorption feature;
- Tomography of the 21 cm line – essentially imaging the Dark Ages period and the distribution of the Hydrogen and matter in the early universe by observing the 21 cm line at different frequencies and hence different times, in this way forming a movie of the evolution of the early universe;
- Power Spectral analysis of the 21 cm line – performing high-resolution analysis of the spatial variations in distribution of the matter in the Dark ages period.

The Global Signal is expected to peak around 30-40 MHz and is weak, ~10^6 below the foreground signal. However, Jester & Falcke (2009) show that even with one dipole antenna (under RFI-low and stable temperature and gain conditions) the signal can be detected at a 5 σ level within integration times in the order of one year, see Figure 3. With DEX the detection of the Global Dark Ages signal is achievable in the order of days, assuming that a full scale DEX array consists of 10^5 individual elements.

As explained by Jester & Falcke (2009), observing the two-dimensional structure of the neutral and reionized hydrogen gas at different frequencies corresponding to different emission redshifts, will provide a tomographic movie of the Dark Ages showing the evolution of the pristine structures in the early universe. This would require DEX to cover the 1-80 MHz regime with arcminute-scale spatial resolution and the ability to detect cosmological milli-Kelvin brightness fluctuations. In Figure 4 (Left Panel) we show the number of dipole antennas required for a 3-σ detection of a 1mK variation in one year of integration time and spatial resolutions of 1' or 10' for different values of the emission redshift. To be able to reach high spatial resolution (1') for instance at z=20 (66 MHz) in the order of 10^7 dipoles are

required and hence a collection area of ~50 km² (see Jester & Falcke, 2009). However, for a spatial resolution of 10', in the order of 10^5 dipoles are required, but more importantly this corresponds to "only" 0.5 km² of collecting area. For z=50, where the 21 cm absorption feature is peaking, a collecting area of ~250 km² (10', one year integration) is required, so at higher values of the redshift the detection of hydrogen variations becomes increasingly difficult but would benefit from longer integration times and higher gain antennas.

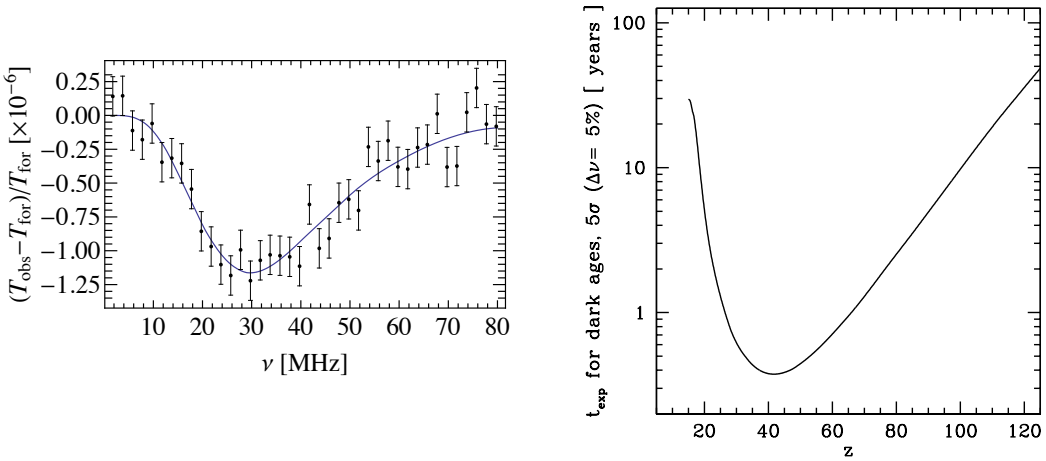

Figure 3: Left Panel: simulation of the 21 cm line after one year of integration for a single sky-limited dipole. Right Panel: Integration times for the 5 σ detection of the 21 cm line for different redshifts. Adding N antennas decreases the integration time with √N. Images adapted from Jester & Falcke (2009).

As pointed out by Loeb & Zaldarriaga (2004) the power spectrum of the redshifted 21 cm line provides cosmological information of higher angular scales of 1' or less and independent samples of the cosmological parameters in the z=30-50 range, compared to the information carried in the CMB. In the right panle of Figure 4 we show the number of dipole antennas necessary to achieve a 5-σ detection of fluctuations in the 21 cm line power spectrum at the mK level for 2' angular resolution for one year of integration, as a function of redshift (see Loeb & Zaldarriaga (2004), Jester & Falcke (2009)). As the signal strength is again in the mK level and the noise is determined by the galactic background noise, the sensitivity and hence the collecting area is again the limiting factor here. For a detection at z=30 and z=50 the number of individual elements is in the order of $10^{5.5}$ and 10^6, which correspond to 3.5 km² and 30 km², respectively. Again, lower collecting area's are required for longer integration times or for lower resolutions. For instance, for 10' angular resolution the collecting areas for z=30 and z=50 correspond to 0.03 km² and 0.28 km², respectively (Jester & Falcke, 2009).

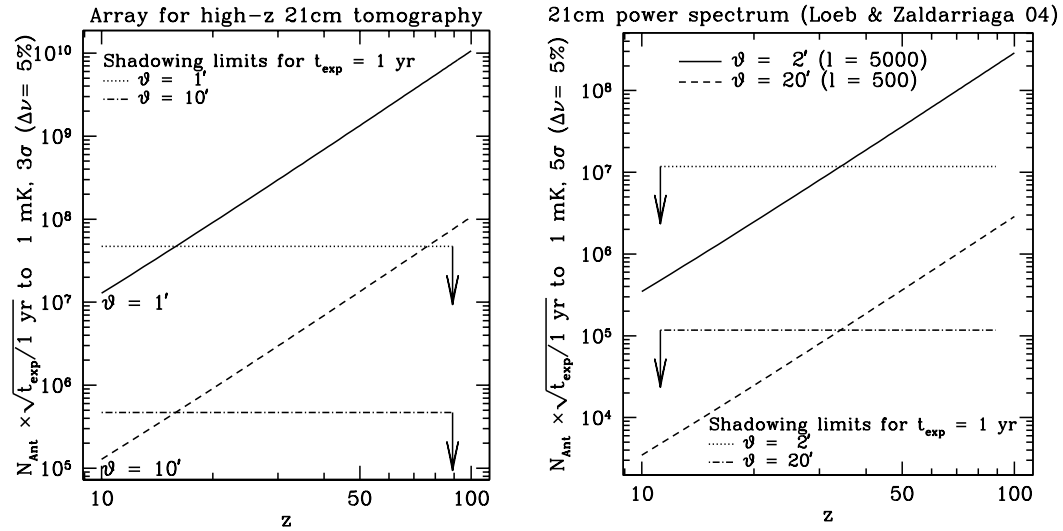

Figure 4: Left Panel: Array size for 21 cm tomography. Right Panel: Array size for Dark Ages power spectrum. Images adopted from Jester & Falcke.

In Figure 5 we show simulated power spectra of the 21 cm line from Pritchard & Loeb (2008); it shows the brightness temperature fluctuations variance integrated over the 3D power-spectrum P(k) in 1 dex shells (hence the $k^2dk \sim k^3$ factor). It reflects the Dark Matter power-spectrum (as the gas follows the Dark Matter at these redshifts), assuming that the spin-temperature follows the temperature of the adiabatically cooling H-I gas. The dashed line corresponds to the DEX array for z=80 (17 MHz; lower panel) and z=40 (34 MHz, top panel). Here we have assumed that we are sky-noise background limited, i.e. the dashed lines in Figure 5 represent the DEX array sensitivity. In this particular example we have taken the DEX array to consist of 10^5 individual dipole antennas, which corresponds to a collecting area of 10 km^2, with an antenna distribution that is constant in a core of 1 km radius
and then falls off as 1/r until 6 km where is becomes zero. The integration time was set to almost one year and the bandwidth was set to 10 MHz. The resulting field-of-view is all-sky. The blue area in the top panel of Figure 5 corresponds to the effective sensitivity of the DEX array: for z=40 it is only limited for the detection of variations on larger scale, by the decrease of strength of the variations (^{10}log(k^{3}P(k)) is close to 0) at ^{10}log(k)=-0.8. For z=80 the DEX array is more limited for detecting variations on all scales as the sensitivity is reduced by about a factor 100, see lower panel Figure 5. From this we conclude that the analysis of the 21 cm power spectra is only meaningful for z<80, hence the lower frequency limit required for the DEX array is ~17 MHz. In addition, Figure 5 shows that for z=40 arcmin scale variations can be achieved for an array with a 10 km^2 collecting area. Again, the collecting area can be reduced either by increasing the integration time, antenna gain (i.e. changing the type of antenna) or the required angular resolution.

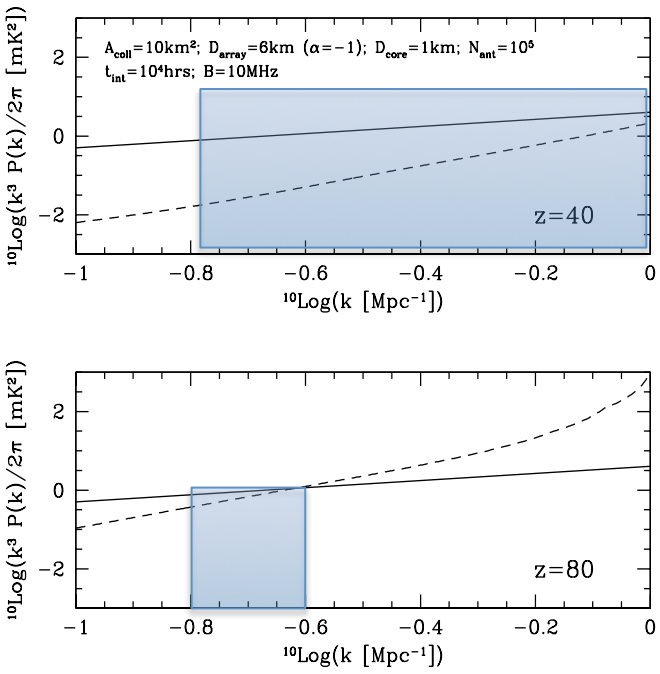

Figure 5: Simulated power spectra of the 21 cm line from Pritchard & Loeb (2008) (solid line) and the expected sensitivity of the DEX array (dashed line) for z=40 (top panel) and z=80 (bottom panel). The blue area corresponds to the effective sensitivity of DEX and hence the range of power spectral variations that can be achieved: for larger values of ^{10}log(k) (to the left on the vertical axis) the corresponding size scales that one can observe is increasing from Mpc scales for ^{10}log(k)=0 to 10 Mpc for -1.

Secondary science cases

Independently from the cosmological breakthroughs that undoubtedly will be achieved in the Dark Ages science, DEX will open up the virtually unexplored low frequency domain below 30 MHz. Like with preceding science instruments that have gained excess to a previously unexplored frequency domain, it is not exactly know which discoveries DEX will provide, but it is unquestionable that they will be made. The low frequency regime corresponds to physical processes that occur at low energies (100 neV – 10 peV) and are associated with relatively large physical scale lengths (several meters to hundreds of km). Hence, it will be in these regimes that DEX will provide new insights and possible scientific breakthroughs. In the following we highlight a number of science topics for which DEX is expected to provide new discoveries.

Non-thermal Planetary Radio Emissions

Planetary magnetospheric emissions

The Earth and the four giant planets in the solar system have magnetospheres, where electrons are accelerated to keV-MeV energies by various processes resulting in intense non-thermal low frequency radio emissions in the auroral regions near and above the magnetic poles. Radio emission is produced at the local electron cyclotron frequency by a resonant mechanism that transfers a fraction of the energy of

the electrons to electromagnetic (radio) waves. This Cyclotron Maser instability (CMI) is a most efficient LF radio generation mechanism and operates at all "radio-planets" (Zarka 1998). The spectral characteristics of all auroral radio emissions predicted for the Lagrange point L2 of the Sun-Earth system are depicted in Figure 6. Jupiter with its 14 Gauss surface magnetic field emits up to 40 MHz, while the other planets only emit below about 1.5 MHz. Most of these emissions occur below the cutoff frequency of the Earth ionosphere. The broadband CMI emissions have a complex (anisotropic) morphology in the time-frequency domain and are tied to the local magnetic field (Fig. 3.5; Zarka et al. 2004).

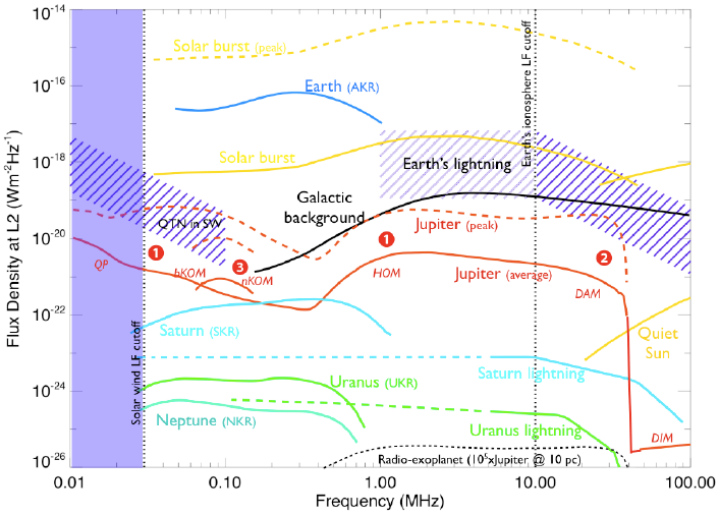

Figure 6: Solar, planetary, and predicted exoplanetary radio emission spectra at the Lagrange point L2 (similar for near-Earth orbit with scaled terrestrial emissions). Numbered features refer to Jovian spectral components depicted in Figure 7: 1) auroral, 2) Io-Jupiter, and 3) Io's plasma torus (Zarka et al. 2008).

Jupiter's radio emissions are intense (MJy), 100% circularly or elliptically polarized, and point-like at a given frequency. Jovian activity is quasi-permanent in the hectometer-kilometer (3-0.3 MHz) range, and reasonably predictable at decameter wavelengths (30 MHz) (Zarka et al., 2004). For all the radio planets, quasi-continuous observations by DEX will allow study of the time variability of the radio emissions, from short pulses to planetary rotation periods, solar wind and satellite modulation. Accurate planetary rotation periods (and phases) determine the atmospheric wind speed and allow merging longitude-dependent data. Modulations due to natural satellites and solar wind strength show magnetospheric dynamics, solar wind - magnetosphere coupling, and electrodynamic coupling of the magnetosphere with satellites. The radio planets are indirect monitors of the solar wind from 1 to 30 AU.

Jupiter serves as an ideal calibration source and a perfect target for cross-calibration or correlation with ground-based observations. DEX imaging mode observations may be used to resolve Jovian emission spread over several radii (Jovian diameter ~40") and science objectives include (Zarka 2004): coarse fast imaging of (moving) sources in the magnetosphere, beaming of the emission and new constraints on the radio generation process, interaction of satellites and the magnetosphere, plasma torus probing (Faraday rotation), and detecting Io's volcanic outbursts.

Based on Figure 6 DEX system can detect the Jupiter and Saturn magnetospheric radio emissions, while The Uranus and Neptune emissions will be detectable when they are in a high state.

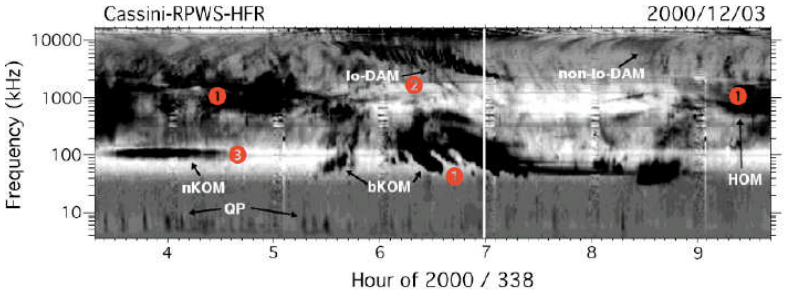

Figure 7: Jovian emissions observed by the RPWS experiment onboard Cassini between 3.5 kHz and 16.1 MHz. Jovian spectral components numbered as in Figure 6 (Zarka et al. 2004).

Exoplanets

Coherent planetary emissions such as Jupiter's are nearly as intense as the radio bursts from the solar corona. Hot Jupiter exo-planets (orbiting at a few stellar radii from their parent star) are predicted to have radio emission up to 10^5-10^6 times the flux of Jupiter if they are strongly magnetized or orbiting a strongly magnetic star or are bombarded by numerous Coronal Mass Ejections from their parent star (Zarka 2007; Greissmeier et al. 2007; Chian et al. 2010). Conservative emission levels are indicated in Figure 6. Hot Jupiter exoplanetary radio emission will be detectable in DEX imaging surveys using long integrations (≥ 12 h) if the emission covers a large bandwidth over

timescales of hours. A premier detection of extrasolar magnetospheric radio emission would confirm the predictions of hot Jupiter sources and would initiate further study of their properties.

Solar Physics and Space weather

Our Sun is a very strong radio source: superimposed on the thermal emissions of the quiet sun are the intense radio bursts that are associated with solar flares and coronal mass ejections (CMEs), clouds of ionized plasma ejected into interplanetary space. Three main types of radio bursts are observed from the Sun particularly in its active state, both related to flares and CMEs. Type II bursts have a frequency drift with time at rates consistent with the speed of the shock through the solar corona and interplanetary medium (~1000-2000 km/s). Type III bursts are emitted by mildly relativistic (~0.1 - 0.3 c) electron beams propagating through the corona and interplanetary space that excite plasma waves at the local plasma frequency. Their frequency drift rate is much higher than that of Type II bursts. Type IV bursts are emitted by energetic electrons in the coronal magnetic field structure (such as coronal loops). Both the Type II and III bursts can be imaged by DEX in the 1-30 MHz range.

The density model of the heliosphere (Mann et al. 1999) directly relates the radio source location (in solar radii) to the emission frequency: higher frequency radio emission originates closer to the surface of the sun, while lower frequency emission originates further out. By providing dynamic spectra and detailed imaging of the solar radio emissions, DEX will allow monitoring and modeling of plasma instabilities in the solar corona and wave-particle interactions in the activity regions of the Sun. In addition, DEX offers great opportunities for radio studies of the solar wind and the heliosphere. It will permit observations of solar radio bursts at low frequencies with much higher spatial resolution than possible from any current or planned space mission. It also allows observations much further out from the solar surface than possible from the ground, where the ionosphere confines the field of view to within a few solar radii. DEX will dynamically image the evolution of CME structures as they propagate out into interplanetary space and potentially impacts on the Earth's magnetosphere.

Transient phenomena

Pulsars are among the best-studied cosmic radio sources. They are quite dim below 30 MHz, and are strongly affected by interstellar dispersion and scattering, but DEX is expected to allow detection of roughly 1% of the 2000 currently known pulsars. This will allow for groundbreaking research into low-frequency pulsar emission, which is not understood. One of the main open questions is the intrinsic bandwidth of pulsar emission. Earth-based observations cut out below 16-18 MHz; only a space-based mission such as DEX can illuminate the low-frequency behavior. Month-long TBM mode integrations can produce folded, coherently de-dispersed profiles for the dozen brightest nearby pulsars in the sky, very similar to the highly successful Fermi gamma- ray mission (Figure 8). These observations will also shed light on the expected change in scattering properties of the ISM at low frequencies, which could be explained by a cutoff in the Kolmogorov turbulence spectrum of the ISM.

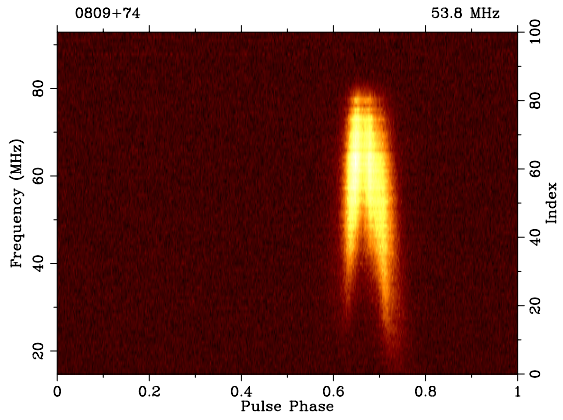

Figure 8: A 1-hr observation of pulsar B0809+74 using a coherent addition of all 24 LOFAR low-band core stations from 15–93 MHz. The data has been de-dispersed and folded using a rotational ephemeris to produce a cumulative pulse profile as a function of frequency. Given that the central observing frequency is 53.8 MHz, the fractional bandwidth is 145%. This wide bandwidth is key to following the drastic evolution of the cumulative profile with frequency. At the bottom of the band there are two distinct pulse components that almost completely merge toward the top of the band (van Haarlem et al. 2013)

The transient radio emission from Gamma-ray bursts (GRBs), supernovae, as well as from accreting black holes, neutrons stars and white dwarfs are all enabled by coherent emission processes. For many of these and similar sources, the emission above 30MHz cannot complete their energy balance. DEX will be the optimal instrument to detect any energy release below 30 MHz, and thus can sample a large discovery

space in RBM or TBM mode observations for fast transients and ASI mode observations for slow transients.

Extra-galactic surveys

high-redshift galaxies and quasars

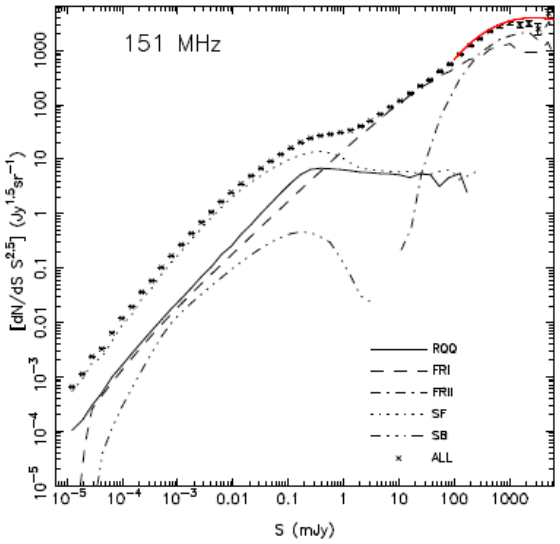

Figure 9: Source counts simulations at 151MHz for different source populations. The red curve shows the currently known counts (Wilman et al. 2008). In the equivalent detection curves at low frequencies, DEX will detect sources down to 200 mJy at 10 MHz and 10 mJy at 30 MHz.

At low radio frequencies, the brightest sources of the extragalactic sky are the nuclei and synchrotron-emitting radio lobes of giant radio galaxies and quasars such as those found in the 3CRR survey (Laing et al. 1983). Multi-frequency radio observations have shown that sources with ultra steep spectra (a < -1.3, where S~na), i.e. relatively bright in the DEX range, are usually hosted by high redshift galaxies (Röttgering et al. 1997). A simple extrapolation from source counts at 74 MHz in the VLSS (VLA Low-Frequency Sky Survey; Cohen et al. 2004) suggests that a DEX survey will discover (at 3s significance) ~2 million sources above the confusion limit of 210 mJy at 10 MHz and of 40 mJy at 30 MHz for a survey time of one year. These source populations occupy the upper end of the flux density distribution similar to the curve depicted in Figure 9. Most of these sources will have relatively steep spectra characteristic of more extended sources rather than the flatter spectra of AGN sources. The survey results are essential for study of the evolutionary history of the different source populations (as in Figure 9). The source catalog will be used to study the spectral properties of specific groups of sources and relate these to their peculiarities.

The source populations that will be detected in such a low frequency survey consist mainly of standard radio galaxies and quasars but will also include other active galaxies (Figure 9). A special class of sources consists of very compact start-up radio galaxies having an active black hole with jets still confined within the recently activated galaxy. Such start-ups are also seen locally (O'Dea 1998) and display a synchrotron self-absorption spectral turnover in the range 100-1000 MHz (Falcke et al. 2004). Some models suggest these to be numerous at redshift 20, where they peak between 5-50 MHz and will be readily identified by a DEX all-sky survey.

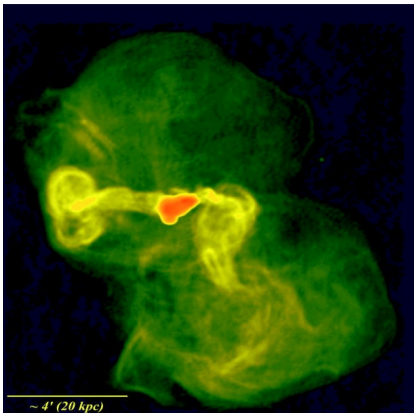

Jet power of radio galaxies

Figure 10: The famous radio Galaxy M87 at a frequency of 74 MHz showing the enormous extent of the lower frequency emission. At higher frequencies only the (orange) central region will be detected (Owen et al. 2000).

The low-frequency emission of radio galaxies and quasars are generated predominantly in the radio lobes. These structures with scales of tens to hundreds of kpc (Begelman et al. 1984) are inflated by relativistic jets symmetrically emerging from the accretion disk around the nuclear black hole of the host galaxy. The lowest-energy electrons in the jets and lobes of these radio galaxies dominate the synchrotron radiation output, which yields the observed steep radio spectra. The shorter cooling time of the higher-energy electrons causes further steepening (spectral ageing) of the radio spectrum in the older parts of a source (Blundell & Rawlings 2001). At the location of the terminal shock front of powerful jets, the "hotspots", the plasma can become optically thick to its own synchrotron emission due to self-absorption. As a result the hotspots frequently show a spectral turnover at frequencies as low as 10 MHz.

From their full size and the turnover frequency, one can deduce reasonable limits of the magnetic fields and mechanical work done by the jet feeding it. In current models of galaxy and black hole formation and evolution (Croton et al. 2006; Hopkins et al. 2007), this AGN feedback is key to regulating both the growth of the accreting black hole and the star formation activity in its host galaxy, giving rise to the old, red stellar populations of massive elliptical galaxies (e.g. Best et al. 2006). DEX observations will constrain the power of the relativistic jet outflows, their physical models, and their interaction with the ISM.

Fossils and AGN feedback

Observations below 30 MHz also probe the oldest structures in a radio galaxy and they provide constraints on their age and the feedback history of the central engine. Radio galaxies and other AGN sources are normal galaxies going through a temporary phase of more or less strong accretion onto their central black hole (Croton et al. 2006). A fundamental issue for interpreting such activity phases is their duration and recurrence timescales. Only for the so-called "double-double" radio galaxies with two sets of double radio lobes (Schoenmakers et al. 2000), this recurrence is directly visible. From synchrotron ageing arguments for these rare sources, both the duration of an activity phase and the recurrence timescale are likely within an order of magnitude of ten million of years.

The spatial extent of (currently) active radio galaxies is much larger at lower frequencies than the structures observed at higher frequencies (600 MHz and above). The gas injected into the lobes by the jets eventually 'cools' and expands into the surrounding medium, creating a low-frequency emission halo as observed in M87 (see Figure 10). However, the emitted power of a radio galaxy decreases as its lobes grow in linear extent. Therefore, only the fairly young radio galaxies (ages $\sim 10^5$-10^7 yr) are observable at high redshifts ($z \gtrsim 0.8$), while at low redshifts they would be observable up to ages of 10^8-10^9 yr (Blundell et al. 1999). Because of this degeneracy, a DEX all-sky search for halo remnants or "fossils" of switched-off (nearby) radio galaxies, will directly address the lifetime and recurrence issues of nuclear activity in radio galaxies.

The only known radio galaxy relics are cool holes in the X-ray emission of the hot cluster gas (see Fabian et al. 2006). This intra-cluster medium (plasma) (ICM) emits (radio) synchrotron radiation, as well as X-rays through inverse-Compton scattering. Existing (and future) all-sky radio observations miss such sources because their observing frequencies are too high to detect these fossil emissions. The time interval for detection after switch-off roughly increases as the inverse of the observing frequency, which is good for a DEX survey. The mechanical energy input into the ICM resulting from AGN activity is important for understanding galaxy formation and ICM thermodynamics. ICM bubbles blown by central engines and 'ghost bubbles' resulting from radio galaxy relics can be detected in X-ray emissions of the nearby Centaurus and Perseus clusters (Fabian et al. 2005, 2006). Such bubbles rise buoyantly in the ICM and are part of the energy transport mechanism in clusters. Analogous to the case of radio galaxies, low-frequency radio observations of clusters will also constrain their energetics, their magnetic fields, their formation history, and the nature of cosmic rays.

The DEX survey observations will discover (hundreds of) thousands of steep-spectrum cluster halo sources during its lifetime, preferentially those of low-mass and high-redshift objects (Cassano et al. 2008). In targeted observations, DEX would detect radio emission from these bubbles and yield stringent constraints on their ages.

Cosmic Rays and High-Energy Neutrino's

Radio emission observed towards Galactic HII regions at low frequencies predominantly arises from material along the line of sight, i.e., the synchrotron emission from cosmic-ray electrons (Duric 2000). Similarly, supernova remnants (SNRs) accelerate high-energy particles through a first-order Fermi shock acceleration mechanism, which only operates on mildly relativistic electrons. Since the frequency of synchrotron emission scales with the particle energy, low-frequency DEX all-sky imaging of visible HII and SNR targets can be used to trace the 3D energy distribution of the lowest-energy particles.

DEX strawman mission concepts

For the definition of the DEX mission concepts we have to take a number of requirements into account that drive the design. The dominant requirements in that respect are the sensitivity and hence collecting area (~10km^2), temperature and gain stability, and RFI-quiet environment. For this reason we consider here two options: a space-based mission and a lunar-farside mission. Although there are essential differences in these two designs, there are also clear similarities. We will therefore first describe a basic (strawman) design that applies to both the space-based and lunar design, and then highlight some of the mission specific design characteristics.

The basic DEX design is that of a low-frequency radio interferometer. DEX will employ the well-tested interferometry techniques to achieve its science objectives. The sensitivity of a radio interferometer with N antenna elements depends on the total number of baselines (relative distance vectors) between pairs of separated antenna elements and scales as $[N\,(N\text{-}1)]^{-½}$. The signals from each pair of elements are cross-correlated and integrated, yielding one (u,v,w) point in the three-dimensional spatial Fourier domain for each sampled baseline and frequency channel. These "snap-shot' correlation data are sent to Earth for offline processing and imaging. For a (to be designed) DEX imaging mode, the bandwidth of the spectral channels is chosen such that the narrow-band condition holds ($\Delta f \leq 1$kHz), thus allowing all-sky imaging. The actual all-sky image is obtained for example by concatenating many small FOV image patches, each obtained from an inverse Fourier transform of the set of sampled (u,v,w) points. The spatial (u,v,w) points for each baseline yield independent (u,v,w) points for each frequency channel ("bandwidth synthesis"). The motions of the individual antennas in space or the rotation of the moon (with respect to the sky), increases the number of unique baselines during the course of the mission, which gradually fills the (u,v,w) volume and greatly improves the quality of the final sky image. In addition, for each combination of three or more elements in the array, self-calibration techniques may be applied that significantly improve the imaging quality. Hence, many elements, large bandwidths, and long integration time generally improve the imaging performance of the interferometer. A second performance figure of an interferometer is its angular resolution, which scales as λ/D, where λ is the observed wavelength and D is the separation distance between antennas. For DEX, angular resolution in the order of 1-10 arcmin will be required for the frequency range between 1-80 MHz. Note that, although the Dark Ages science is limited to the 17-80 MHz regime, we have chosen DEX to be sensitive in the 1-80 MHz regime to allow for additional science (i.e. auroral emission from planets, see Figure 6).

The DEX science objectives will be addressed using three basic operational modes:

- **Wide Band Spectroscopy mode**: runs continuously in parallel with any of the other modes, and produces one time averaged complex spectrum at full bandwidth every 5 minutes. This mode is particularly designed for study of the highly redshifted 21-cm signal during the Dark Ages over the full 0.1-80 MHz range.
- **All-Sky Imaging mode**: employs the imaging capability of the full antenna array and allows imaging of the whole sky at the spatial resolution afforded by the array. The nominal bandwidth correlated by the system is 10 MHz and the centre frequency of the observations can be selected across the whole 70 MHz frequency range of the system. The complete auto- and cross-correlation matrix data will be produced as 1-10 sec records for further calibration and image processing. Correlation is done in narrow-band frequency channels, thus allowing all-sky imaging. Ground-based processing of the cross-correlation data will allow calibration and imaging of the whole sky, while the auto-correlation data provides the signal integrated over the whole sky.
- **Burst mode**: employs beamforming to phase up the array for a particular target area. Spectral data will be produced at significantly faster sampling time as low as 50 ms for further ground-based processing. This mode will be well suited for sensitive observations of pulsars, transients, and variable planetary emissions.

In Figure 11 we provide the data acquisition system design that will be very similar for both the space- and moon-based option, as they address the same science. The difference between these two options lies in the way the data is processed and transformed, as will be discussed in the next sections.

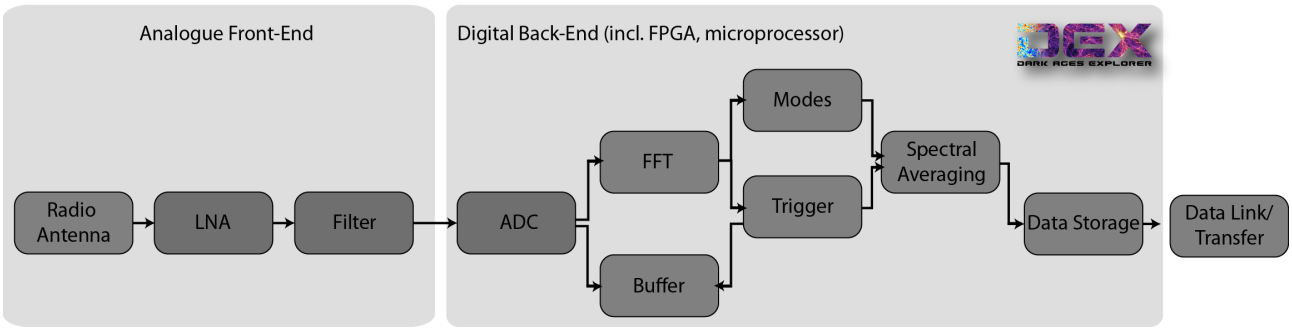

Figure 11: DEX data acquisition design. The modes correspond to the science operational modes as described in the text.

Space-based mission: Swarms of nano-satellites

The main design considerations for an astronomical low-frequency array in space relate to the physical characteristics of the interplanetary and interstellar medium. The configuration of the satellite constellation and the achievable communication and processing bandwidths in relation to the imaging capabilities are also crucial design considerations. The system will consist of a swarm of 10^5 identical satellites (sensors) spread over kilometric distances that will orbit faraway from terrestrial radio frequency interference. The distributed solution should provide redundancy and robustness, as it is insensitive to failure or non-availability of a small fraction of its components.

Using current-day technologies, a space-based low-frequency array would be bulky and, thus, costly. A logical next step would be to miniaturize the electronics and use very small satellites, perhaps even nano satellites with masses between 1-10 kg to build the radio telescope. The approach is to use a swarm of satellites to establish a virtual telescope to perform the astronomical task. In recent studies, such as DARIS (Saks et al., 2010) and FIRST (Bergman et al., 2009) it is shown that with extrapolation of current signal processing and satellite technologies, a low frequency radio telescope in space could be feasible in the coming years. DARIS has already shown that a 9-satellite cluster, with a centralized system can be implemented in moon orbit with today's technology.

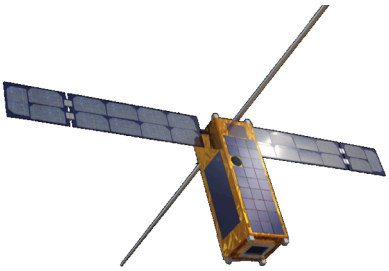

Figure 12: OLFAR antenna and platform concept; i.e. one swarm element.

To enlarge the cluster, the satellites must be smaller. The OLFAR project (Bentum et al., 2009; Rajan et al., 2011; Engelen et al., 2010) aims to develop a detailed system concept and to design and build scalable autonomous satellite flight units to be used as an astronomical instrument for low frequencies. To achieve sufficient spatial resolution, the minimum distances between the satellites must be more than 10 km and due to inter stellar scattering this maximum baseline is limited to 100 km, giving a resolution of 1 arc minute at 10 MHz. The OLFAR 3-dimensional cluster will comprise of 50 - 1000 satellites, each containing a dipole (or tripole) antenna (Figure 12), observing the sky from 0.3-30MHz. The satellites will employ passive formation flying and yet maintain sufficient position stability for a given integration time. In the presence of a stable orbit and thus stable baseline, position estimates can be more precisely known and thus the integration time can be extended up to 1000 seconds and thereby reducing the down-link data rate. For astronomical observations, mechanical dishes will be very expensive in terms of mass, power and operation. Instead OLFAR satellites will use a relatively simple antenna.

Each individual satellite will consist of deployable antennas. The sky signals will be amplified using an integrated ultra-low power direct sampling receiver and digitizer. Using digital filtering, any subband within the LNA passband can be selected. The data will be distributed over the available nodes in space. On-board signal processing will filter the data, invoke RFI mitigation algorithms (if necessary), and finally, correlate the data in a phased array mode. If more satellites are available, they will automatically join the array. The final correlated or beam-formed data will be sent to Earth as part of the telemetry data using a radio link. As the satellites will be far away from Earth, communication to and from Earth will require diversity communication schemes, using all the individual satellites together.

Based on previous designs for space-based, low-frequency, interferometry missions such as DARIS (Daris, 2010), SURO, HEIMDAL, DARE (Burns et al. 2012) and OLFAR (Olfar 2012) we summarize the DEX space-based mission design as follows:

- The individual antennas are omni-directional tripoles (active antennas), with their sensitivity optimized in the 1-80 MHz regime. For the secondary science cases the lower limit of this range can possibly be extended downwards to 0.1 MHz.
- The antennas are mounted on nano-satellites that provide power (solar panels) and basic processing (FFT and averaging algorithms) and communication.
- The array is build up from these individual antennas and together with a mothership that provides data storage, processing and communication with Earth, it acts as a swarm. This means that the individual antennas are interchangeable, and that each antenna should now its position but that the array is not controlled from a central hub. Due to the motion of the individual antennas, the baselines are constantly changing and complete coverage of the (u,v,w) plane is achieved.
- The array should be placed in a RFI-quiet location, for instance at the Sun-Earth L2 point or in an Earth-leading or Earth-trailing orbit. This will minimize the need for RFI-mitigation techniques.
- Each individual antenna should be calibrated carefully and the noise pattern (EMC) should be characterized in detail.
- Data processing can be done at a central mother-ship which has dedicated data processing facilities, more power available (larger solar sails) and large data rate available for data transfer, the individual antenna then have to transfer the data to the mothership and have to perform some on-board processing to reduce the data volume somewhat;
- Alternatively, data processing and transfer can be arranged by the array of antennas, i.e. they act as a swarm. This has the advantage that with the increase of the array the processing power is increased, but also requires each individual element to be provided with significant processing and communication capabilities;
- For the communication between the individual antennas and the mothership, optical communication and nano-photonics can be used;
- Optionally, the individual antenna can based on inflatable space structures, see the discussion below.

Inflatable space structures

DEX requires a significant collecting area (10 km^2) and while the radio antenna and receiver technologies are well developed (TRL levels of 6 and higher), bringing them into space or to the moon is a costly and technologically challenging endeavor. In order to reduce the weight, the mechanisms required for the deployment and hence the costs of such a mission, we suggest the use of inflatable space structures. Already since mid 20th century inflatable space structures are being used to bring sizable structures in space, and the first two missions launched by NASA in 1960, Echo 1 and 2, were successfully used as communication reflectors for transmission of radio signals (telephone, radio and television signals) from one point to another on Earth. For this reason they were operated in the MHz regime. At the end of the 20th century interest in inflatable space structures was renewed which resulted in the successful deployment of the NASA Inflatable Antenna Experiment (IAE) from space shuttle mission STS-77 in 1996 (Freeland et al., 1997). In addition, a number of mission concepts where proposed, for instance QUASAT which is an ESA/NASA concept for a free-flying VLBI antenna with a spaceborn 15m reflector which operates at 1.6, 5 and 22 GHz. For DEX the inflatable space structure technology can be adapted for the platform or deployment of the antenna system, comparable to the IAE concept, see Figure 13.

As an alternative for the traditional tripole radio antenna design, inflatable balloon structures can be considered. For instance, the 10 km^2 required for DEX can be obtained by forming an array of 300 Echo 2 antennas. Given the current development in the commercial space flight (SpaceX, Biggalow Aerospace, Virgin Galactic, XCOR) the deployment and realization of DEX is becoming feasible in the near future from a technological and financial point-of-view.

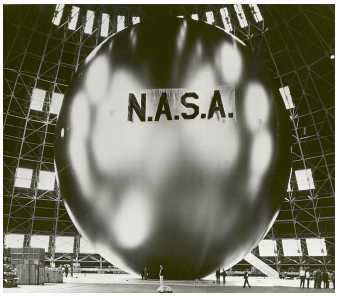

Figure 13: Left Panel: Echo 2 satellite (1960). The balloon was made of metalized PET film, had a diameter of 41.1 m and a mass in the order of 180-200 kg. Right Panel: the NASA IAE launched from the space shuttle in 1996.

Moon-based mission: LOFAR on the moon

The moon, and in particular the lunar far-side, has already for many years been considered to be the most ideal location for low-frequency radio astronomy (e.g. Basart & Burns, 1990). Not only has the moon no atmosphere or significant ionosphere it can also provide significant attenuation (40 dB or more) of man-made RFI signals and locations with stable temperature and gain conditions. In the past several lunar mission concepts have been suggested, some proposing more "traditional" designs using tripole antennas such as the LRX instrument on the European Lunar Lander, see Klein Wolt et al., 2012, while others propose to use innovative and lightweight designs, such as the ROLSS mission proposed by NASA (see Burns et al. 2009; Lazio et al., 2011). But these concepts differ also in other respects. While LRX consists of one single, omni-directional active antenna (kHz-100 MHz range), the ROLSS concept consists of 500m long arms forming a Y-shape on the lunar surface, with each arm having 16 antennas. The arms are made of thin polyimide and the antenna is operational in the 1-10 MHz regime reaching less than 2° resolution at 10 MHz. In addition, note that both concept are addressing different science. In any case, both the LRX and ROLSS should be considered path-finder missions for future large arrays, such as the Dark Ages Lunar Interferometer (DALI, see Lazio et al. 2007) which is a concept very similar to DEX.

The DEX lunar concept design on the one hand draws from the previous proposed lunar mission concepts, but on the other hand will be based on the experience and expertise gained with Earth-based low-frequency interferometers such as LOFAR and in the future SKA. In particular the experience in the technical realization of a large collecting area radio array in (often) remote locations, calibration of the instruments, RFI mitigation techniques and the handling and processing of large data volumes is essential for the development of DEX. In short, the DEX lunar interferometer design has the following characteristics:

- Interferometer array, consisting of $\sim 10^5$ individual antenna elements together realizing a ~ 10 km^2 collecting area on the lunar surface, sensitive in the 1-80 MHz frequency regime.
- The individual antenna elements can consist of traditional dipole or tripole antennas (e.g. LRX, see Klein Wolt et al. 2012) or be placed on thin metal sheets that are rolled out on the surface (ROLSS, see Lazio et al. 2011).
- The location should be chosen carefully in order to provide temperature and gain stability as well as attenuation of RFI signals from Earth and Solar activity, preferred is the lunar far-side but South- or North Pole locations using shielding from mountains is also an option. Note that while the lunar far-side is preferred, it does require an additional orbiter for communication to the Earth.
- At a Lunar far-side location the data processing and communication should be done from the orbiter: it provides more power from solar panels and has better communications with Earth available compared to stationary platforms on the lunar far-side.
- Each individual antenna should be calibrated carefully and the noise pattern (EMC) should be characterized in detail.

Long-term focus

The realization of a 10 km^2 DEX interferometer in space or on the moon is a significant technological challenge that should be approached in a step-wise fashion and depends on future developments in the areas of space transportation, light-weight inflatable space structures, data communication and low-power-high-performance data processing and swarm technologies. Both concepts presented are based on the same science case and have communalities with respect to the data processing and operational modes, but also are equally flexible and scalable. In both cases individual elements can be added to the array which would increase the sensitivity and science output, and in some cases also the total data

processing capabilities. Starting a small-size DEX array, as a path-finder mission, would also immediately provide valuable science output; not only would the DEX path-finder open up the last unexplored frequency domain, but it would allow for the detection of the global Dark Ages signal as well address many of the secondary science cases (planetary radio emission, all sky survey etc).

As mentioned above, a lunar location is much preferred from a scientific point of view but also from an explorational point of view. The realization of a space-based DEX array at for instance Sun-Earth L2 could be considered as a single-shot mission that would be difficult to "share" with other potential users, while a DEX array on the moon would provide a basic infrastructure that would allow other scientific or explorational benefits and could be considered as a long-term investment. Note that, a lunar location would also allow DEX to address a number of additional science that was not mentioned here, for a detailed overview see Klein Wolt et al., 2012.

Finally, scientifically the DEX interferometer is the natural next step. On the one hand it is the successor of the earth-based low frequency interferometers such as LOFAR and SKA, opening up the last unexplored frequency regime for astronomy, which is *not* possible from earth-based antennas. On the other hand DEX's unique and unprecedented detailed view of the evolution and structure formation of the very early universe (Dark Ages and Cosmic Dawn) will help cosmologist to constrain the models and predictions that are coming from the WMAP and PLANCK missions that study the CMB.

TRL levels

Here we provide an estimate of the expected increase in the TRL levels in the 2013-2030 timeframe for some of the key technologies that will be used by DEX.

Technologies	Current TRL	Expected TRL @ L2- L3	Expected critical developments
Radio Antenna (lightweight, foldable, inflatable)	5	6-7	Small, foldable light-weight structures are being designed in the OLFAR and ROLSS project that should fit a nano-satellite.
Radio Receiver (low-power, high processing, 200 MHz receivers)	5-6	6-7	Prototype radio receivers are expected to be tested in rocket flights in the near future, and similar systems will be tested in space environments (e.g. ISS). Further heritage is gained from ground-based low-frequency instruments such as LOFAR, SKA, MWA, LWA and space-based instruments such as LRO
Digital processing system	4-5	6-7	Development of power-saving and smart algorithms to processes large quantities of data with significantly less power are currently ongoing in many Big-Data Science projects (CERN, ITER, LOFAR, SKA)
Optical communication	6-8	7-9	Optical communication and nano-photonics are expected to be employed in space industry (telecom) and has been tested since the 1970s (e.g. SILEX on ESA Artemis)
Swarm Technologies	3-4	5-6	OLFAR, inter-satellite communication, satellite control
Thin-film solar panels	4-5	7-8	Currently thin-film solar panels are considered for future missions with expected launch dates before L2 and L3
Radio Frequency interferometry	7-9	7-9	Based on space-ground interferometers (HALCA and RadioAstron), and there's been some crude time-difference-of-arrival measurements (interferometric-like) using the THEMIS or Cluster spacecraft.
Inflatable space structures	7-8	8-9	NASA Echo1 and 2 missions, NASA inflatable antenna experiment (IAE, 1996)

Conclusions

The Dark Ages eXplorer, DEX, is a low-frequency radio interferometer in space or on the moon, that will probe deep into the early universe and provide an unprecedented detailed view of the evolution of the first structures in the universe. DEX is sensitive in the 1-80 MHz regime which allows a complete view of the Dark Ages and Cosmic Dawn period, essentially covering the z=17-80 redshift regime (Figure 14). DEX will explore the Dark Ages and the Cosmic Dawn and observe the global neutral hydrogen (21 cm) emission and its variations on arcmin scales in order to constrain cosmological models on the evolution of the early universe, the onset of the epoch of reionization and basically constrain the models and predictions that will follow from the Planck mission and address the following science questions:

SQ1 When did the Cosmic Dawn occur and which sources are responsible for the onset of the Cosmic Dawn?
SQ2 How did the first sources form?
SQ3 What was the impact and feedback of the first sources on the IGM?
SQ4 What is the spectrum of the Global Dark Ages signal and how does is change over time / redshift?
SQ5 What is the tomography of the Global Dark Ages signal?
SQ6 What is the scale of the density fluctuations in the early universe?
SQ7 How does the Dark Matter couple to the IGM/gas?
SQ8 What is the cooling rate of the early universe (Dark Ages)?

These issues form the *holy grail of cosmology* and the Dark Ages is the treasure-trove for Dark Matter and Early universe physicists.
In addition, DEX will open up the last virtually unexplored frequency regime below 30 MHz, extending the view of LOFAR and SKA to the ultra-long wavelength regime that is not accessible from Earth, and among a wealth of science cases will provide high resolution low-frequency sky maps, constrain models on the jet power in radio galaxies, observe auroral emission from the large planets in our solar system and possibly find Jupiter-like exoplanets.
DEX requires a large collecting area in the order of 10 km^2 (10^5 individual elements) and a location (preferably the lunar far-side) that provides shielding from man-made radio interference (RFI), absence of ionospheric distortions, and high temperature and antenna gain stability. The realization of large collecting area interferometers has been achieved on earth already (e.g. LOFAR and in the near future SKA) and the technique behind it is well developed (TRL 4-5). The realization in space or on the moon is a very challenging task. However, we are convinced that given the technology developments, especially in the areas of nano satellites, RF technology and low-power and high-performance computing, the construction of a large low-frequency radio array in space or on the moon is feasible in the 2020-2030 timeframe.

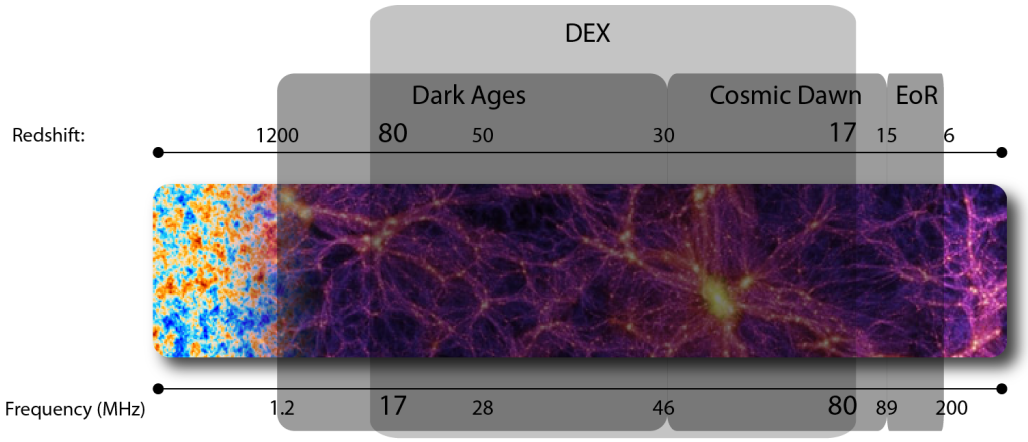

Figure 14: The DEX frequency regime. The lower limit of 17 MHz is only for the Dark Ages science. We have chosen the 1-80 MHz band to allow for additional science.

References

Barkana & Loeb, 2006, MNRAS, 372, 43

Begelman, M.C., Blandford, R.D., & Rees, M.J., 1984, Rev. Mod. Phys. 56, 255

Bentum et al., 2009, *60th International Astronautical Congress, Daejeon, Republic of Korea, 12 – 16 October, 2009*.

Bergman et al., 2009, ArXiv e-prints

Best, P.N. et al., 2006, MNRAS, 368, L67

Blundell, K.M., Rawlings, S., & Willott, C.J., 1999, AJ 117, 677

Blundell, K.M. & Rawlings, S., 2001, PASP Conf 250, 363

Braude et al., 2002, IAUS, 199, 490

Burns et al., 2009, AAS, 213, 451.03

Burns et al., 2012, AdSpR, 49, 433

Burns, J.O. et al. 2012, AdSpR 48, 1942

Cassano et al., 2008, A&A, 480, 687

Cane & Whitham, 1977, MNRAS, 179, 21-29

Cane & Erikson, 2001, Radio Science 36, 1765-1768

Carilli et al., 2007, Proceedings of the workshop "Astrophysics Enabled by the Return to the Moon". Cambridge University Press, in press astro-ph/0702070

Chian, A.C. et al., 2010, Adv. Space Res., 46, 472

Ciardi, B., & Ferrara, A. 2005, Space Science Rev., 116, 625

Cohen, A.S., et al., 2004, ApJS, 150, 417

Croton, D.J., et al., 2006, MNRAS, 365, 11

DARIS, 2010, *Very Large Effective Receiving Antenna Aperture in Space*, ESTEC/Contract 22108/08/NL/ST

Duric, N., 2000, in *Radio Astronomy at long wavelengths*, Stone, R.G., et al. (Eds.), 277

Ellis & Mendillo, 1987, Australian Journal of Physics 40, 705–708.

Engelen et al., 2010, *24th Annual Conference on Small Satellites, Utah, USA, August 9-12. 2010*

Fabian, A.C., Sanders, J.S., Taylor, G.B., & Allen, S.W., 2005, MNRAS 360, L20

Fabian, A.C., et al., 2006, MNRAS 360, L20

Falcke, H., Körding, E., & Nagar, N.M., 2004, NewAR 48, 1157

Farrell et al., 1999, JGR, 14025-14032

Freeland et al., 1997, IAF-97, 1.3.01

Griessmeier, J.M., et al. 2007, PSS, 55, 618

Hopkins, P.F., Richards, G.T., & Hernquist, L., 2007, ApJ, 654, 731

Jester, S., & Falcke, H., 2009, NewAR, 53, 1

Kassim & Weiler, 1990, Proceedings of an International Workshop, Crystal City, VA, Jan. 8, 9, 1990.

Klein Wolt et al., 2012, P&SS, 74, 167

Kraus, 1986, "Radio Astronomy Receivers", Powell, Ohio: Cygnus-Quasar Books, 1986

Lazio et al., 2011, Advances in Space Research 48, 1942–1957.

Lazio J. et al., 2007, AAS, 39, 135

LOFAR, 2012, The Low Frequency Array, www.lofar.org

Loeb & Zaldarriaga, 2004, PhRvL, 92u, 1301

Mann et al., 1999, A&A, 348, 614

Novaco & Brown, 1978

O'Dea, C.P., 1998, PASP, 110, 493

Owen, F., Eilek, J. & Kassim, N., 2000, ApJ 514, 611

Pritchrd & Loeb, 2008? Of 2010?

Pritchard & Loeb, 2010, Nature 468, 772-773

Rajan et al., 2011, *IEEE Aerospace Conference, Montana, US, March 5-12 2011*

Rees, 1999, Vol. 470 of American Institute of Physics Conference Series. pp. 13–+

Röttgering, H.J.A., et al., 1997, A&A, 326, 505

Saks et al., 2010, *The 4S Symposium, Madeira, Portugal, 31 May - 4 June 2010*

Schoenmakers et al., 2000, MNRAS, 315, 371

Tseliakhovich & Hirata 2010

Van Haarlem et al., 2013, accepted for A&A, arXiv, 1305.3550

Weiler, 1987, Proceedings of the Workshop, Green Bank, WV, Sept. 30-Oct. 2, 1986

Weiler et al., 1988, A&A, 195, 372-379

Wilman et al., 2008, MNRAS, 388, 1335

Zarka, 1992, AdSpR, 12, 99

Zarka et al., 2004, Journal of Geophysical Research (Space Physics) 109 (A18), 9

Zarka, P., 1998, J. Geophys. Res., 103, 20159

Zarka, P., 2004, Planet. Space Sci., 52, 1455

Zarka, P., 2007, Planet. Space Sci., 55, 598

Zarka, P., Cecconi, B. & Kurth. W., 2004, J. Geophys. Res., 109, A09S15

Zarka, P., Farrell, W., Fischer, G. & Konovalenko, A., 2008, Space Sci. Rev., 137, 257